ANL/CP--73338

DE91 014007

Temperature Dependence of the Elastic Behavior of Structurally Disordered Metallic Superlattices*

J. A. Jaszczak and D. Wolf
Materials Science Division
Argonne National Laboratory
Argonne, Illinois 60439

MAY 1991

DISCLAIMER

*JAJ was supported by the Office of Naval Research under Contract No. N00014-88-F-0019. DW was supported by the U.S. Department of Energy, BES Materials Science, under Contract No. W-31-109-Eng-38. This work was supported in part through a grant of computer time from the National Energy Research Supercomputer Center.

Manuscript being submitted for publication in the Proceedings of the Materials Research Society 1991 Spring Meeting (Volume 229), Anaheim, California, April 29-May 3, 1991.

TEMPERATURE DEPENDENCE OF THE ELASTIC BEHAVIOR OF STRUCTURALLY DISORDERED METALLIC SUPERLATTICES

J. A. JASZCZAK AND D. WOLF
Materials Science Division, Argonne National Laboratory, Argonne, Illinois 60439

ABSTRACT

The structure and elastic properties of superlattices composed of high-angle twist grain boundaries on (100) planes of copper are investigated as a function of both the modulation wavelength and temperature via molecular dynamics simulations. Comparison is made with zero-temperature results, where a stiffening of the Young's modulus normal to the interfaces and a softening of the modulus for shear parallel to the interfaces has previously been observed. The differences between the effects of homogeneous (temperature-induced) and inhomogeneous (interface-induced) structural disorder on the elastic properties is explored.

INTRODUCTION

The elastic anomalies of metallic superlattices, including a strengthening of certain moduli and a softening of others, have been the subject of investigation of numerous experimental [1-9] and theoretical studies [10-13]. In particular, the anomalous enhancements of Young's and biaxial moduli (supermodulus effect) [1,5-8] at small modulation wavelengths, Λ, (defined in Fig. 1) have motivated continued research in hopes of being able to engineer desired elastic properties into layered materials.

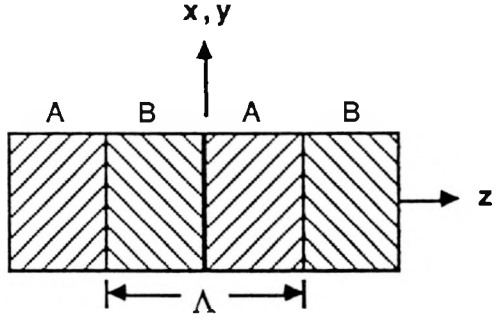

Fig. 1. Periodic arrangement of materials A and B forming a superlattice modulated along **z**. The modulation wavelength is Λ. In the grain-boundary superlattices of this study, A and B are the same material, but rotated with respect to each other about the (001) plane normal ($\|\mathbf{z}$) to form a periodic array of high-angle twist grain boundaries.

A series of computer simulations of well-characterized metallic superlattices at zero temperature has helped to elucidate the origin of the elastic anomalies. Perfectly coherent (strained-layer), composition-modulated superlattices, with very little structural disorder at the interfaces, have been studied in a number of papers [17-21], and have shown little or no anomalous elastic behavior. However, incoherent superlattices, with significant structural disorder in the form of misfit dislocations at the interfaces, have shown an enhancement of the Young's and biaxial moduli, as well as a softening of the moduli for shear parallel to the interfaces [20-21]. Larger elastic anomalies in the incoherent superlattices have been correlated to greater structural disorder via a larger lattice-parameter mismatch [20-21]. Incoherent, composition-modulated superlattices with alternating materials rotated with respect to each other about the interface normals, have also been studied. These superlattices, with the largest degree of structural disorder at the interfaces of the systems studied, showed greatest elastic anomalies [21].

Grain-boundary superlattices (GBSLs), composed of a periodic arrangement of high-angle twist grain boundaries (Fig. 1), also show enhancements in the Young's and biaxial moduli, and a softening of the shear moduli [13-15]. These simple model systems show an excellent correlation between the amount of structural disorder at the interfaces and the degree of the elastic anomalies [16], and are appropriate model systems for disordered composition-modulated superlattices [21]. These studies have made it clear that the supermodulus effect is primarily an interface effect whose magnitude is controlled by the degree of inhomogeneous structural disorder and the anharmonicity of the potential, but not the homogeneous (albeit anisotropic) lattice-parameter changes.

In this study we further investigate the different, and sometimes competing effects of inhomogeneous and homogeneous disorder on elastic behavior by investigating the effects of

temperature on GBSLs and perfect crystals under conditions of constant stress and also constant volume. Whereas thermal vibrations increase the degree of homogeneous structural disorder and might be expected to lead to elastic strengthening, under constant-stress conditions there are subsequent lattice-parameter increases which ultimately lead to elastic softening. We choose, for this study, GBSLs composed of high-angle twist grain boundaries (GBs) on (001) planes of an fcc metal, with a twist angle of 36.87° [the so-called Σ5 (001) symmetrical twist grain boundary]. Such GBSLs are advantageous for study since they are relatively simple systems, they exhibit interesting elastic anomalies even at zero temperature, and they are directly comparable to perfect crystals of the same material. Furthermore, they are appropriate models for disordered, composition-modulated metallic superlattices [21] and possibly nanocrystals [22].

SIMULATION METHOD

In many of the previous simulation studies of supermodulus behavior, both Lennard-Jones (LJ) and embedded-atom-method (EAM) [23] potentials were used for comparison. Although the LJ potential satisfies the Cauchy relation at zero temperature, both the LJ and EAM potentials yield qualitatively the same physical behavior in these systems. Consequently, for this study we have chosen a LJ potential fitted to have the zero-temperature lattice parameter (a=3.616Å) and zero-pressure melting temperature of copper (approximately 1200K) by choosing the usual LJ parameters to be σ=2.3151Å and ε=0.167 eV [24]. To avoid discontinuities in the energies and forces, the potential was smoothly shifted to zero at the cut-off radius of 1.49a. Zero-temperature structures with various numbers of (001) planes between GBs (and thus various Λ values) were relaxed under zero applied stress using an iterative energy-minimization technique with strictly three-dimensional periodic border conditions [25]. In the present study, the simulation cell contained 20 atoms per (001) plane to prevent atoms from interacting with themselves through the periodic borders. In the previous studies of the (001) GBSLs, the average elastic-constant tensors were calculated at zero temperature via a lattice-dynamics method that included the "relaxation term" arising from the intrinsic inhomogeneities of the superlattices [14,15,26]. In this study, the structures and elastic properties at non-zero temperatures were obtained by constant-temperature molecular dynamics (MD) simulations, where the temperature was adjusted by uniform velocity rescaling. The time step used was $0.05\sigma(m/\varepsilon)^{1/2}$ (0.0018 psec.). Equilibrated structures at each temperature were used as input structures for the next higher temperature. For each value of Λ and T, the unit-cell dimensions under zero-stress conditions were first determined by constant-stress equilibrations of 10,000 time steps. The unit-cell dimensions were then fixed for the elastic-constant determinations.

The isothermal elastic constants were determined for both perfect crystals and GBSLs using the so-called fluctuation formula [27,28]. Averages were computed over anywhere from 40,000 to 190,000 time steps, depending on the system. For testing and later comparison with GBSLs, the temperature dependence of the elastic constants of a perfect fcc crystal with, 108 atoms in the simulation cell, under zero stress was evaluated via the fluctuation formula. As expected, under zero stress the elastic constants show a dramatic softening with increasing temperature (by over 60% at 1000K).

Since in principle, the fluctuation formula, is not strictly applicable to inhomogeneous systems, we have tested its validity by determining the elastic constants from stress-strain curves for the highly inhomogeneous GBSL consisting of four (001) planes between GBs at T=100K. These stress-strain curves were computed via MD simulation by applying a series of fixed strains, from -0.001 to +0.001, to the simulation cell, while monitoring the resulting stresses. The latter were averaged over 15,000 to 25,000 time steps after an initial 5,000 to 10,000 time-step equilibration under the applied strain. A comparison of the fluctuation-formula results with stress-strain results shows that elastic constants C_{ij}, for $i,j \leq 3$, can reliably be calculated by the fluctuation formula to within 1% or better. Other elastic constants could not reliably be calculated via the fluctuation formula for reasons which are as yet unclear, and are therefore not presented in the following discussion.

RESULTS

For each value of the modulation wavelength and temperature, a GBSL was equilibrated under zero applied stress, and the average lattice parameters were determined. The anisotropic thermal expansion of one superlattice is illustrated in Fig. 2, which shows the average lattice

parameter normal (a_z) and parallel (a_x) to the interfaces. The isotropic thermal expansion of the lattice parameter of a perfect crystal is shown for comparison. As one might expect from the enhanced anharmonicity associated with the large volume expansion at the GBs at zero temperature, the thermal expansion of a_z is 50% larger than that of a_x. Also, due to the expanded and disordered interfaces, a_x itself shows an almost 200% larger thermal expansion than that of a perfect crystal.

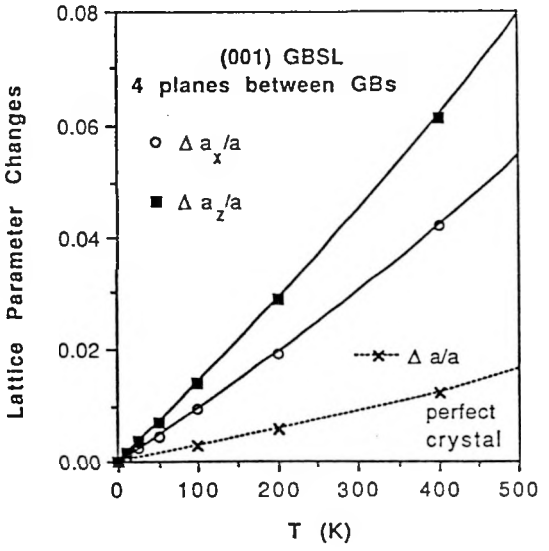

Fig. 2. Thermal expansions of the lattice parameters parallel (a_x) and perpendicular (a_z) to the interfaces in an (001) GBSL of four planes between GBs. Shown for comparison (dashed line) is the thermal expansion of the perfect-crystal lattice parameter. All changes in lattice parameters are normalized to the zero-temperature lattice parameter.

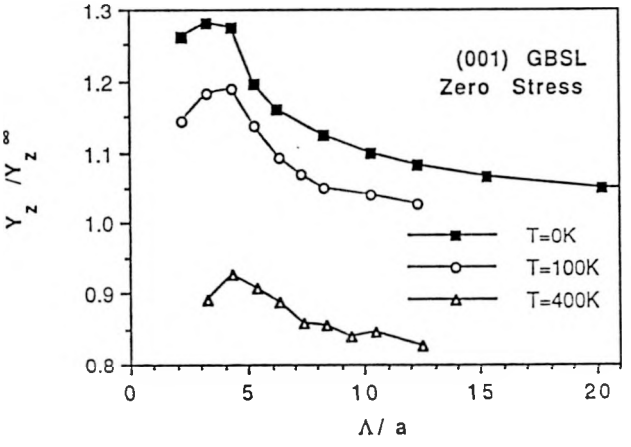

Fig. 3. Isothermal Young's modulus Y_z, as a function of Λ at T=0, 100 and 400K. The biaxial modulus and C_{33} behave similarly. The values are normalized to the T=0 values in the $\Lambda\rightarrow\infty$ limit (Table I).

Table I. Selected zero-temperature elastic constants and moduli (in units of 10^{12}dyn/cm^2) for a perfect fcc crystal and for the GBSLs in the $\Lambda\rightarrow\infty$ limit, using the Lennard-Jones Cu potential. For the perfect crystal, the x, y and z axes are aligned with the <001> symmetry axes. For the GBSL, z is parallel to [001], while the x and y axes are rotated from the symmetry axes by half the CSL angle (i.e. 18.44°).

Elastic Constant or Modulus	(001) Grain-Boundary Superlattice in the $\Lambda\rightarrow\infty$ limit
$C_{11} = C_{22}$	2.025
C_{12}	0.789
$C_{13} = C_{23}$	1.016
C_{33}	1.808
$C_{44}=C_{55}=G_{xz}=G_{yz}$	1.016
Y_{bz}	1.681
Y_z	1.076

The variation of a representative elastic modulus, Y_z, with temperature and modulation wavelength is shown in Fig. 3, normalized to the corresponding value in Table I. Immediately

clear is that even at non-zero temperatures, the GBSLs show the same generic behavior as a function of Λ as they did at zero temperature. In particular, despite the large thermal expansions, there remains an enhancement, at small Λ, of the Young's modulus, Y_z (Fig. 3), biaxial modulus, Y_{bz}, and elastic constant C_{33}, over their respective values at large Λ. The in-plane Young's moduli, $Y_x=Y_y$, and elastic constants, $C_{11}=C_{22}$, show only a softening with decreasing Λ. However, for a fixed Λ, and therefore fixed inhomogeneous structural disorder, the effect of increasing the temperature at zero stress is to soften all moduli and elastic constants.

DISCUSSION

By normalizing the results in Fig. 3 to the corresponding finite-temperature values of Y_z in the $\Lambda\rightarrow\infty$ limit, instead of those at T=0, it becomes evident (see Fig. 4) that the effects of the thermal disorder and subsequent volume expansion largely soften the elastic moduli by the same degree, independent of the amount of inhomogeneous structural disorder (i.e. Λ). The most inhomogeneous systems (at smaller Λ), however, do soften faster than those at larger Λ.

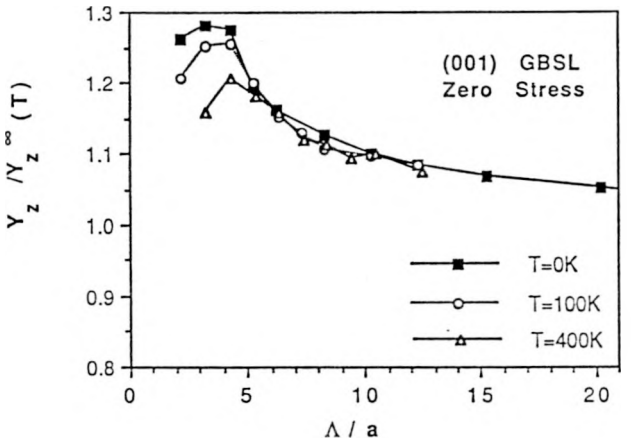

Fig. 4. Isothermal Young's modulus Y_z as a function of Λ at T=0, 100 and 400K. The moduli are here normalized to their $\Lambda\rightarrow\infty$ limit values at the same temperature: $Y_z^{\infty}(T)$=1.0762, 1.0199, and 0.8264 $\times 10^{12}$ dyn/cm^2 at T=0, 100, 400K, respectively.

In order to further compare the effects of temperature on the GBSLs and perfect crystals, Fig. 5(a) illustrates the radial distribution function, G(r), for both a perfect crystal and a GBSL composed of four (001) planes between the GBs at T=400K. As noted earlier, this GBSL shows the most anomalous elastic behavior (see Fig. 3). While the centers of the GBSL peaks are at the same positions as the perfect crystal peaks, the GBSL peaks are slightly broader. Indicative of the structural disorder, the GBSL shows a significant number of pair separations distinct from perfect-crystal separations. With increasing temperature under zero stress, the GBSL peaks broaden further and shift to larger separations [Fig. 5(b)], similar to behavior in perfect crystals.

As shown in Fig. 6, the combined effects of the broadening and shifting of the peaks in G(r) on the elastic constants and moduli of the GBSLs is a linear softening with increasing temperature, just as for a perfect crystal. Since the broadening of these peaks should lead to a stiffening of certain elastic moduli, while the volume expansion induced shifts in the peaks should cause a softening [13], it is of interest to deconvolute these two competing effects induced by increasing temperature. This is easily accomplished by fixing the simulation-cell size to that corresponding to zero stress at T=0. Due to the system's anharmonicity, this results in an increase in the stresses with increasing temperature. The radial distribution functions at fixed volume are very similar to those at zero stress, showing a broadening of the peaks with increasing temperature, but not a shift in the peaks to larger separations with increasing temperature. As shown in Fig. 7, there is indeed a slight strengthening of Y_z over the zero-temperature value with increasing temperature due to the thermal disorder. The strengthening over the zero-stress-state values at the same temperature, however, is quite significant, and is due to the constraint of no volume expansion.

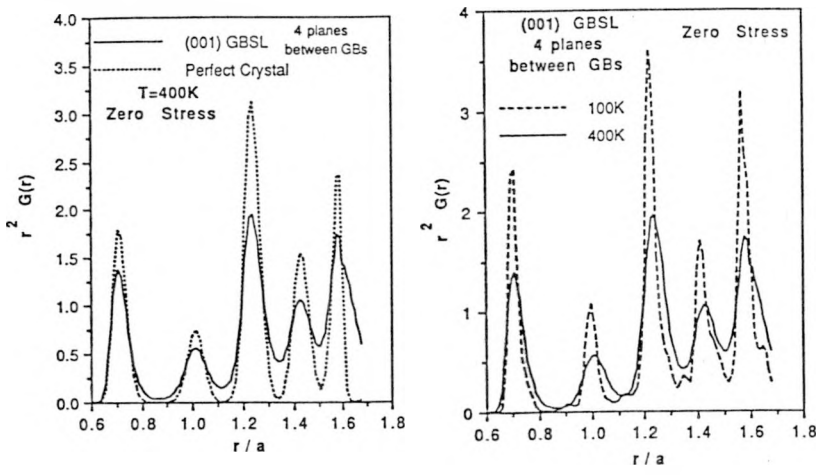

Fig. 5. Radial distribution function of (a) a perfect crystal and a GBSL with four (001) planes between GBs at T=400K and zero stress, and (b) the same GBSL at T=100 and 400K under zero stress. G(r) is normalized such that at T=0 the nearest-neighbor peak would be a delta function of height 12 for the perfect crystal.

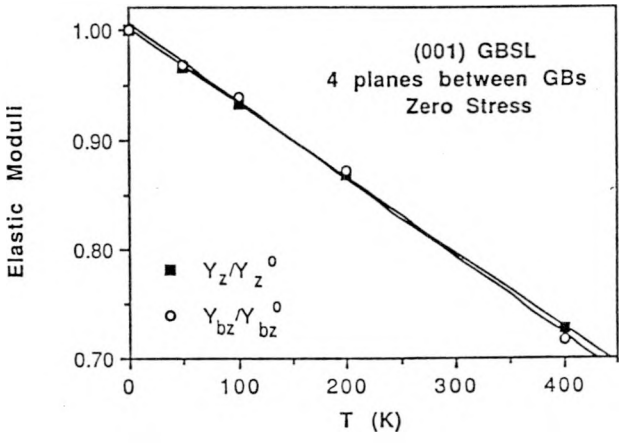

Fig. 6. Selected isothermal elastic moduli as a function of temperature of a GBSL composed of four (001) planes between GBs under zero stress. The elastic constants C_{11} and C_{33} soften similarly. Moduli are normalized to the T=0 values for this GBSL: $Y_z^o=1.371\times10^{12}$ dyn/cm^2, and $Y_{bz}^o=1.873\times10^{12}$ dyn/cm^2.

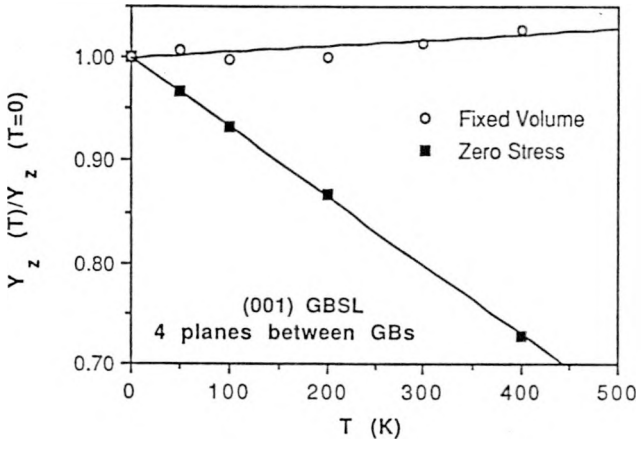

Fig. 7. Isothermal Young's modulus, Y_z, as a function of temperature of a GBSL with four (001) planes between GBs under zero stress (open circles) and also at the volume fixed to the T=0 zero-stress volume (solid squares). The the biaxial modulus and the elastic constant C_{33} behave similarly. Values are normalized to the zero temperature values, as in Fig. 6.

ELASTIC STRENGTHENING OF PERFECT CRYSTALS?

The competing thermal effects of broadened G(r) peaks and the shifting of their centers to larger separations should also be observed in the elastic properties of perfect crystals under zero stress. The radial distribution function of a perfect fcc crystal under zero stress shows both a broadening and a shifting of the peaks with increasing temperature. The overall effect on the elastic behavior is a softening of all of the elastic constants with increasing temperature (by over 60% at 1000K). Based on the GBSL results, however, we expect that if the volume were held fixed to the T=0, zero-stress volume, even the perfect crystal should show elastic stiffening with increasing temperature due to the disorder. Indeed, at fixed volume the elastic constants C_{11} and C_{12} of a perfect crystal are enhanced up to 8% at T=1000K over the T=0 values, and all three elastic constants are enhanced over the zero-stress values at a given temperature.

CONCLUSIONS

By investigating the elastic behavior of superlattices of grain boundaries as a function of temperature under both constant stress and constant volume conditions, we have shown that

structural disorder and volume expansion play competing roles in the "supermodulus effect". Whereas the structural disorder, be it inherent (inhomogeneous) or due to thermal fluctuations (homogeneous), can lead to a stiffening of certain elastic properties, subsequent volume expansions under constant-stress conditions lead to elastic softening. By suppressing the volume expansion in both perfect crystals and in grain-boundary superlattices, we have shown that thermal disorder, like inhomogeneous structural disorder, can cause elastic stiffening. Volume expansions do not always dominate over disorder, however, as is evident by the enhanced moduli of small-Λ, highly inhomogeneous, disordered metallic superlattices.

The inherently inhomogeneous grain-boundary superlattices respond in a homogeneous (perfect-crystal-like) fashion with the introduction of homogeneous (thermal) disorder under both constant-stress and constant-volume conditions. Their anomalous elastic behavior as a function of Λ, i.e. the amount of inhomogeneous structural disorder, persists even at non-zero temperatures. Under zero stress, however, the smaller-Λ superlattices soften slightly faster than the larger-Λ superlattices with increasing temperature.

We have benefitted from discussions with S. R. Phillpot and J. M. Rickman. This work was supported in part through a grant of computer time from the National Energy Research Supercomputer Center. JAJ was supported by the Office of Naval Research under Contract No. N00014-88-F-0019. DW was supported by the U.S. Department of Energy, BES Materials Science, under Contract No. W-31-109-Eng-38.

REFERENCES

1. W. M. C. Yang, T. Tsakalakos, and J. E. Hilliard, J. Appl. Phys. **48**, 876 (1977).
2. I. K. Schuller, in *The Institute of Electrical and Electronics Engineers Ultrasonics Symposium, 1985*, edited by B. R. McAvoy (IEEE, New York, 1985), p. 1093; I. K. Schuller, A. Fartash, and M. Grimsditch, MRS Bull. **XV** (10), 33 (1990).
3. M. H. Grimsditch, in *Topics in Applied Physics: Light Scattering in Solids V*, edited by M. Cardona and G. Guntherodt (Springer-Verlag, Berlin, 1989), p. 285.
4. B. M. Clemens and G. L. Eesley, Phys. Rev. Lett. **61**, 2356 (1988).
5. U. Helmersson, S. Todorova, S. A. Barnett, and J. E. Sundgren, J. Appl. Phys. **62**, 481 (1987).
6. G. E. Henein and J. E. Hilliard, J. Appl. Phys. **54,** 728 (1983).
7. T. Tsakalakos and J. E. Hilliard, J. Appl. Phys. **54,** 734 (1983).
8. J. R. Dutcher, S. Lee, J. Kim, G. I. Stegeman, and C. M. Falco, Phys. Rev. Lett. **65**, 1231 (1990).
9. B. M. Davis, D. N. Seidman, A. Moreau, J. B. Ketterson, J. Mattson and M. Grimsditch, Phys. Rev. B **43**, 9304 (1991).
10. W. E. Pickett, J. Phys. F **12**, 2195 (1982); T. B. Wu, J. Appl. Phys. **53**, 5265 (1982).
11. A. I. Jankowski and T. Tsakalakos, J. Phys. F **15,** 1279 (1985).
12. A. I. Jankowski, J. Phys. F **18**, 413 (1988).
13. D. Wolf and J. F. Lutsko, Phys. Rev. Lett. **60**, 1170 (1988).
14. D. Wolf and J. F. Lutsko, J. Appl. Phys. **66**, 1961 (1989); D. Wolf and J. F. Lutsko in *Metal-Ceramic Interfaces*, edited by M. Ruhle, A. G. Evans, M. F. Ashby, and J. P. Hirth (Permagon Press, Oxford, 1990), p. 52.
15. D. Wolf and J. F. Lutsko, J. Mater. Res. **4**, 1427 (1989).
16. D. Wolf, Mat. Sci. Eng. **A126**, 1 (1990).
17. S. R. Phillpot and D. Wolf, Scripta Metall. Mater. **24**, 1109 (1990).
18. B. W. Dodson, Phys. Rev. B **37**, 727 (1988).
19. J. W. Mintmire, Mater. Sci. Eng. **A126**, 29 (1990).
20. J. A. Jaszczak, S. R. Phillpot, and D. Wolf, J. Appl. Phys. **68**, 4573 (1990).
21. J. A. Jaszczak and D. Wolf, J. Mater. Res. (in press).
22. See, for example, R. W. Siegel, MRS Bull. **XV** (10), 60 (1990).
23. M. S. Daw and M. I. Baskes, Phys. Rev. B **29**, 6443 (1984).
24. J. F. Lutsko, D. Wolf, S. R. Phillpot, and T. Nguyen, Phys. Rev. B **38**, 11572 (1988).
25. D. Wolf, Acta Metall. **32**, 245 (1984); Acta Metall. **37**, 1983 (1989).
26. J. F. Lutsko, J. Appl. Phys. **65**, 2991 (1989).
27. J. Ray, Computer Physics Reports **8**, 111 (1988).
28. D. R. Squire, A. C. Holt, and W. G. Hoover, Physica **42**, 388 (1969).